*Essential Readings in Light Metals: Alumina and Bauxite.*
Edited by Don Donaldson and Benny E. Raahauge.


Light Metals — From *Light Metals 1987*, R.D. Zabreznik, Editor

# FACTORS AFFECTING THE ATTRITION STRENGTH OF ALUMINA PRODUCTS

J.V. Sang

Alcan International Limited
Kingston Research and Development Centre
P.O. Box 8400
Kingston, Ontario
Canada K7L 4Z4

The attrition strength of alumina is a matter of increasing interest. The aim of the present paper is to show how the strength of alumina is related to the precipitation parameters and to the morphology of the precursor hydrate particles.

It is shown that the strength of the product alumina depends on the mode of growth of the hydrate; strong final products are obtained at high liquor supersaturations, conducive to growth by a surface nucleation mechanism which tends to fill the space between crystallites with a "cementing" layer of hydrate. Therefore, strong products are obtained under conditions which increase the supersaturation level - i.e. low precipitation temperatures, high initial ratios and decreased caustic concentrations.

## INTRODUCTION

During the past decade several changes in the alumina industry eg. stationary calciners, point feeding of pots and dry scrubbing systems, have required an increase in the size of the hydrates and/or aluminas. The general result has been a reduction in liquor productivity.

To minimize such loss in productivity, the strength of the hydrate and/or alumina has become a new dimension of the Bayer precipitation process. Previous work on the subject[1,2] has related particle strength to particle morphology: strong particles generally consist of a core of agglomerated particles which have been subsequently cemented together by growth. However the optimum conditions for this strengthening growth are not well defined[3]. It is the objective of this paper to show how the strength of the product is related to the precipitation parameters.

## EXPERIMENTAL

Batch precipitation tests were carried out in 1-litre precipitation bottles filled to 750 ml and rotating end over end at 12 rpm in a water bath. The temperature of the water bath was controlled by a temperature programmer from Eurotherm Corporation. Unless otherwise specified precipitation time was set at 24 hours and the seed charges maintained at 150 g/L. Continuous precipitation tests were carried out in the equipment described in a previous paper[4].

In all tests a plant Bayer solution was used. Its composition* was adjusted to the required caustic concentration by adding caustic pellets. The ratio was adjusted by digesting hydrate. Precipitation yields were determined by filtering the solids, followed by washing, drying at 100°C and weighing. Particle size distribution of the hydrate products was determined with the Wagner turbidimeter. From the obtained size analysis the number of particles per gram of material was calculated by assuming that the particles are spherical:

$$N(\text{Number/litre}) = \sum_{r=1}^{12} \frac{6\times10^{12}\ f}{\pi\ d_r^3\ \rho} \qquad (1)$$

where $d_r$ is the size range 10, 20...120 μm and f is the number density of particles within this size range while ρ is the specific gravity (i.e. 2.4 g/cm$^3$).

The net generation of particles per litre of liquor was calculated by:

$$\left|\begin{matrix}\text{Net generation of}\\ \text{particle (Number/L)}\end{matrix}\right| =$$

$$\left|\begin{matrix}\text{Product}\\ \text{(g/L hydrate)}\end{matrix}\right| \cdot \left|\begin{matrix}\text{Number of particles}\\ \text{per gram in product}\end{matrix}\right| \qquad (2)$$

$$- \left|\begin{matrix}\text{Seed Charge}\\ \text{(g/L)}\end{matrix}\right| \cdot \left|\begin{matrix}\text{Number of particles}\\ \text{per gram in seed}\end{matrix}\right|$$

The aluminas tested were produced by calcining very rapidly the corresponding hydrates. This was achieved by charging the hydrates into a monel beaker (12.5 cm diameter, 20 cm height) which was placed in a preheated furnace. The corresponding heating rate was found to be rapid since the equilibrium temperature, e.g. 1000°C was reached within 5 min.

* In accordance with North American Bayer Plant practice, alumina concentrations are expressed throughout as g/L $Al_2O_3$ and caustic soda concentrations as g/L equivalent $Na_2CO_3$.

The amount of -45 μm material generated in the Forsyth-Hertwig attrition test[5] of both hydrate and alumina was measured by wet sieving. The attrition index was calculated as follows*:

$$\text{Attrition Index} = \frac{\%\text{-45 μm after attrition} - \%\text{-45 μm before attrition}}{100 - \%\text{-45 μm before attrition}} \times 100 \quad (3)$$

It was found that unlike the attrition index on the hydrate, the attrition index on the laboratory calcined hydrate provided a good measure of the attrition occurring in a full scale fluid-flash calciner: analysis of plant data gathered over an 8-month period shows that the following relationship applies with a correlation coefficient of 0.98:

$$\text{Percent Variation in -45 μm (kiln product to kiln feed)} = 0.74 + 0.46 \times (\text{Attrition Index})_{\text{lab calcined}} \quad (4)$$

## RESULTS

In the first series of tests we investigated how precipitation conditions affect the attrition strength of the products obtained from a single precipitation. In the second series of tests the effects of consecutive coarsening cycles and of product size were investigated.

### Effect of Precipitation Conditions

The effect of the alumina supersaturation on the attrition strength of precipitation products can best be demonstrated by continuous precipitation tests performed at constant supersaturation levels. Our tests consisted of growing a narrow size fraction (45 to 74 μm) of a plant seed at two sets of constant supersaturation levels corresponding to ratios of 0.600 and 0.370 respectively. In both cases the precipitation was continued until a target median size of 90-95 μm was obtained. This required 5.6 and 1030 hours respectively.

Table 1. Attrition Strength as a Function of Supersaturation (Continuous Precipitation Tests)

| Ratio | Precipitation Time (h) | Median Size (μm) | | Attrition Indices (%) | |
|---|---|---|---|---|---|
| | | Seed | Product | Hydrate | Alumina |
| 0.370 | 1030 | 60 | 91 | 4.8 | 54.0 |
| 0.600 | 5.6 | 61 | 93 | 1.1 | 10.1 |

* Standard deviation on the attrition indices on the hydrate and alumina were 0.1% and 0.25% respectively.

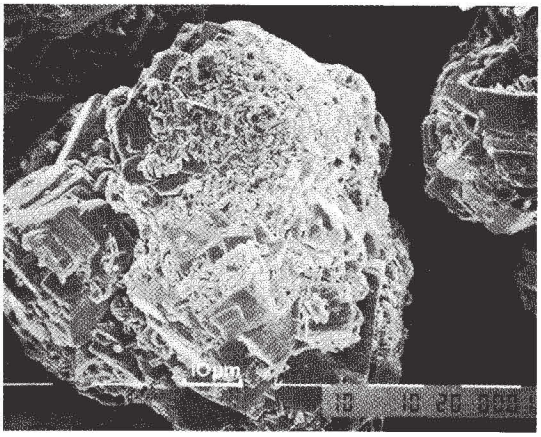


(A)

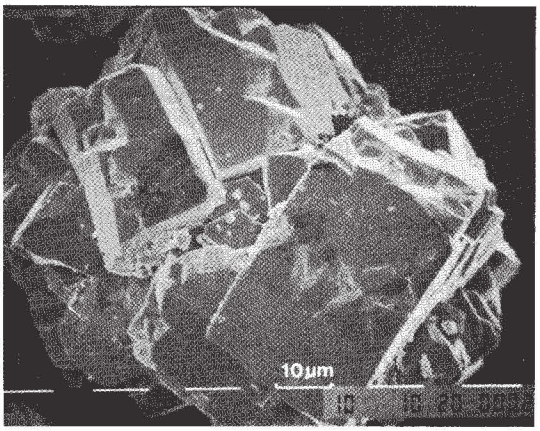


(B)

Figure 1. Scanning Electron Photomicrographs of Products Obtained at Constant Ratio (a) 0.600 Ratio (b) 0.370 Ratio.

The results of the attrition tests reported in Table 1, show that the attrition index on the calcined product obtained at low ratio is considerably higher than that on the product obtained at high ratio, i.e. 54% vs 10%. Scanning electron photomicrographs presented in Figure 1, show that growth at low supersaturation results in bulky monocrystals while growth at high supersaturation results in much smaller monocrystals.

The controlling effect of the alumina supersaturation on the attrition strength of the precipitation product is also demonstrated by the evolution of product strength during batch precipitation cycles carried out at different temperatures. Results reported in Table 2 and illustrated in Figure 2 show that a maximum product strength is achieved with only a small fraction of the total precipitate coming down in the early stages of the precipitation cycle, i.e. maximum attrition strength on the calcined product is attained after 1 hour at 74°C, 2 hours at 68.5°C and 4 hours at 62.8°C. It can be seen in Table 2, that such increase in the strengthening period with decreasing precipitation temperature

Table 2. Attrition Strength as a Function of Precipitation Time and Precipitation Temperature

| | | | | | | | | | |
|---|---|---|---|---|---|---|---|---|---|
| Case I. Initial Precipitation Temperature 74.8°C (Cooling 0.30°C/h) | | | | | | | | | |
| Precipitation Time (h) | 0 | 0.25 | 0.50 | 0.75 | 1.0 | 2.0 | 4.0 | 7.0 | 24.0 |
| Supersaturation ($g/L\ Al_2O_3$) | 49.2 | 47.2 | 40.0 | 35.5 | 31.1 | 23.1 | 15.1 | 11.1 | 6.3 |
| Attrition Indices (%) | | | | | | | | | |
| Hydrate | 11.7 | 10.7 | 7.4 | 7.4 | 6.3 | 6.7 | 7.2 | 7.2 | 8.2 |
| Alumina | 36.3 | 31.1 | 24.5 | 21.8 | 20.6 | 20.7 | 20.7 | 23.1 | 22.6 |
| Case II. Initial Precipitation Temperature 68.5°C (Cooling 0.3°C/h) | | | | | | | | | |
| Precipitation Time (h) | 0 | 0.25 | 0.50 | 0.75 | 1.0 | 2.0 | 4.0 | 7.0 | 24.0 |
| Supersaturation ($g/L\ Al_2O_3$) | 56.6 | 53.4 | 47.5 | 42.6 | 40.2 | 32.0 | 23.4 | 17.5 | 12.0 |
| Attrition Indices (%) | | | | | | | | | |
| Hydrate | 11.7 | 11.0 | 8.8 | 7.9 | 7.7 | 7.1 | 6.7 | 7.1 | 7.2 |
| Alumina | 36.3 | 29.8 | 25.7 | 22.8 | 22.9 | 20.5 | 20.3 | 21.4 | 21.6 |
| Case III: Initial Precipitation Temperature 62.8°C (Cooling 0.3°C/h) | | | | | | | | | |
| Precipitation Time (h) | 0 | 0.25 | 0.50 | 0.75 | 1.0 | 2.0 | 4.0 | 7.0 | 24.0 |
| Supersaturation ($g/L\ Al_2O_3$) | 64.2 | 62.5 | 58.4 | 54.4 | 50.4 | 42.1 | 32.5 | 25.5 | 17.3 |
| Attrition Indices (%) | | | | | | | | | |
| Hydrate | 11.7 | 11.9 | 8.7 | 7.3 | 7.6 | 6.0 | 5.9 | 6.0 | 4.9 |
| Alumina | 36.3 | 32.8 | 25.9 | 22.9 | 20.2 | 18.8 | 16.9 | 18.0 | 17.1 |

is related to the respective supersaturation levels, i.e. $Al_2O_3$ concentrations above equilibrium concentrations. Strengthening occurs only when the supersaturation level is above 30-32.5 g/L. Therefore, by depressing the alumina equilibrium concentrations lower temperatures tend to extend the strengthening period.

It thus appears that there is a minimum supersaturation level required for strengthening. Such supersaturation threshold levels can be related to the growth process itself and particularly to growth by a surface nucleation mechanism at high liquor supersaturations. As shown in Figure 3, small crystallites are generated only during the first hours of the precipitation cycle at a precipitation temperature of 74°C. However, as shown in Figure 4, at a precipitation temperature of 62.8°C the generation of new crystallites occurs for periods up to 4 hours. These small crystallites generated during the period of high supersaturation tend to fill up the voids between the grains and thereby increase the strength of the product. At lower supersaturation levels, however, no more new crystallites are formed and only the existing crystals grow. Such subsequent growth does not strengthen the product and can even result in weaker product.

Results reported in Table 3 show that at constant initial alumina/caustic ratio the attrition strength of the resulting hydrate and alumina decrease as the caustic concentration is increased from 190 to 250 g/L. As expected, and as evidenced by the population balances, this decrease in attrition strength is associated with a decrease in secondary nucleation rates. The SEM photomicrographs attached in Figure 5, indicate that less surface nucleation occurs on the surface of the crystals when the caustic concentration is increased.

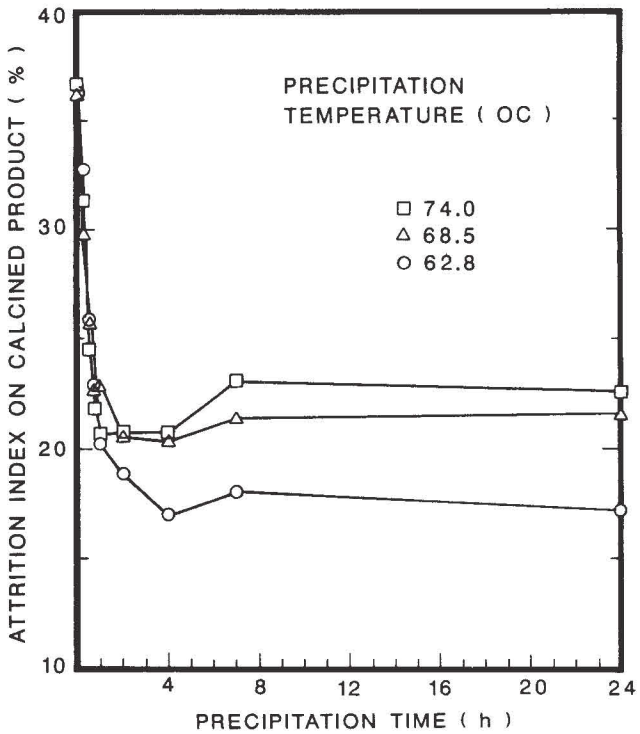


Figure 2. Attrition of Calcined Product as a Function of Precipitation Time and Precipitation Temperature.

It has been shown that the attrition strength of the product increases with the initial ratio. It can be expected therefore that the decrease in product strength with increasing caustic concentration could be counteracted by an increase in the initial ratio. As shown in Table 4, tests carried out at a caustic concentration of 250 g/L

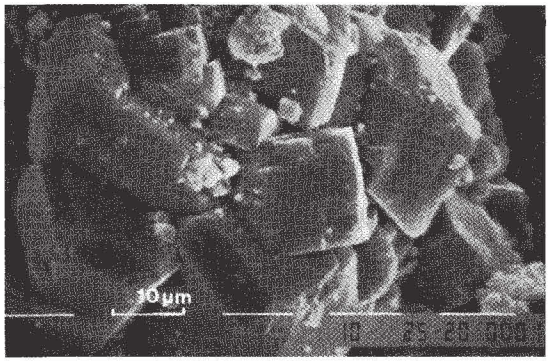


0.5 hour

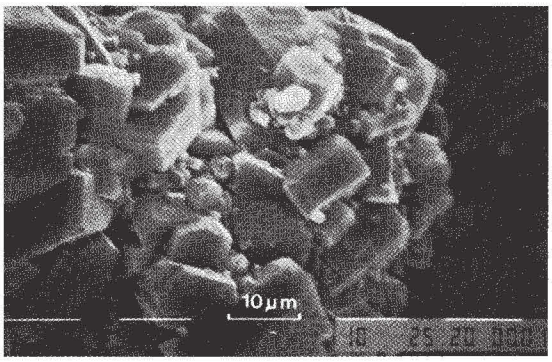


1 hour

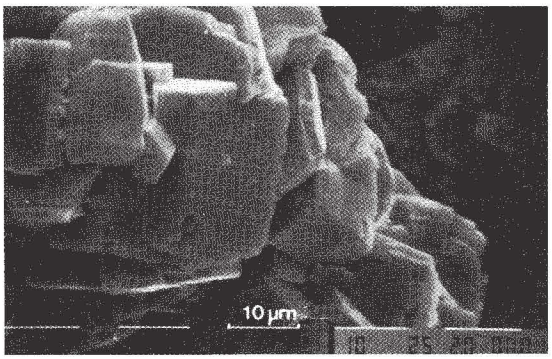


2 hours

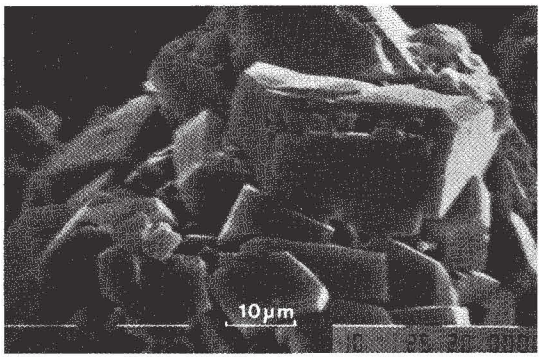


4 hours

Figure 3. Evolution of Products Precipitated at 74°C

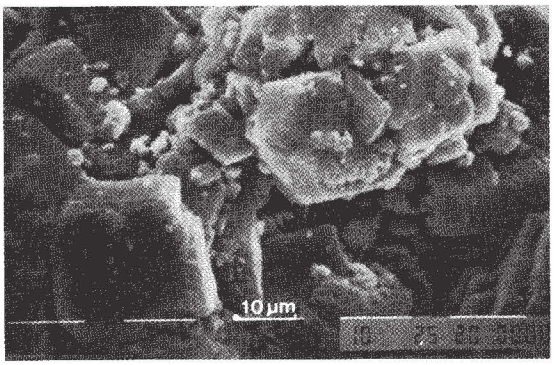


0.5 hour

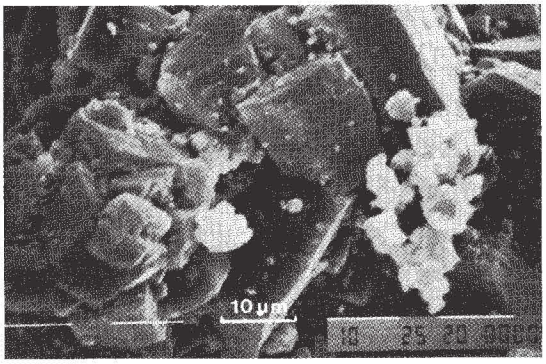


1 hour

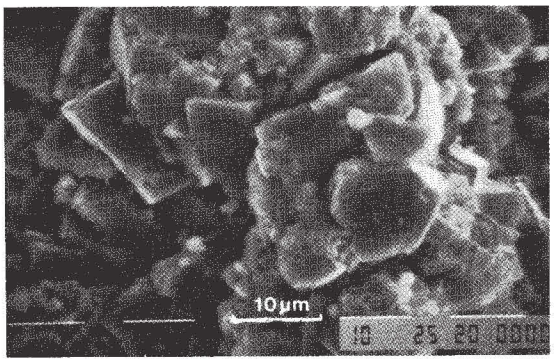


2 hours

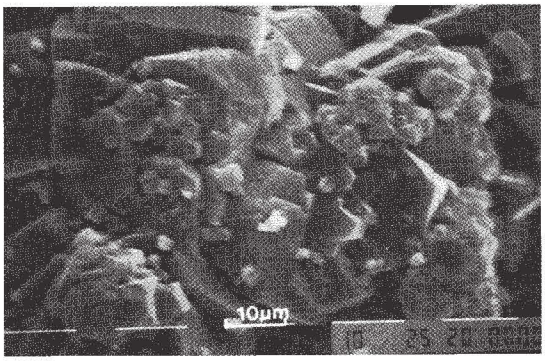


4 hours

Figure 4. Evolution of Products Precipitated at 62.8°C

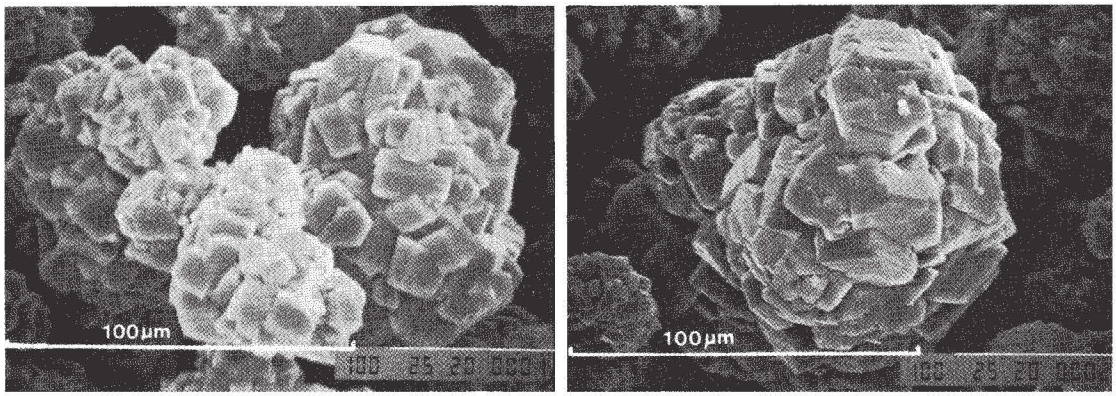


(A) (B)

Figure 5. Products Obtained at Low and high Caustic Concentrations (a) 190 g/L Caustic (b) 250 g/L Caustic.

Table 3. Attrition Strength as a Function of Caustic Concentration (Constant Ratio 0.650)

| | | | |
|---|---|---|---|
| Caustic | 190 | 225 | 250 |
| Yield (g/L $Al_2O_3$) | 58.1 | 61.1 | 60.4 |
| Population Balances | | | |
| N/g × $10^{-6}$ | 5.0 | 3.4 | 3.3 |
| N/L × $10^{-6}$ | 40 | -330 | -360 |
| Attrition (%) | | | |
| Hydrate | 5.4 | 7.1 | 7.9 |
| Alumina | 15.8 | 19.6 | 22.0 |

Table 4. Attrition Strength as a Function of Initial Ratio (Constant Caustic 250 g/L)

| | | | |
|---|---|---|---|
| Initial Ratio | 0.650 | 0.700 | 0.750 |
| Yield (g/L $Al_2O_3$) | 60.4 | 74.3 | 88.0 |
| Population Balances | | | |
| N/g × $10^{-6}$ | 3.3 | 3.4 | 3.7 |
| N/L × $10^{-6}$ | -360 | -260 | -100 |
| Attrition (%) | | | |
| Hydrate | 7.9 | 6.7 | 5.2 |
| Alumina | 22.0 | 19.2 | 16.1 |

and at ratios varying between 0.650 to 0.750 confirm this point. Comparison of results reported in Tables 3 and 4 indicate that to maintain product strength when increasing the caustic concentration from 190 g/L to 250 g/L would require an increase in the initial ratio from 0.650 to 0.750.

Effect Of Consecutive Coarsening Cycles and Of Product Size

In the previous section we have investigated how the precipitation conditions affect the attrition strength of the products obtained in one single precipitation cycle. In the plant, however, the agglomerated seed is recycled many times in consecutive growth cycles. This number of passes in the coarsening stages, depends on the circuit arrangement and on the operation of the classification circuit.

The effect of consecutive coarsening cycles on the attrition strength of product was evaluated by recycling a narrow size fraction, i.e. 45×74 µm of a plant seed in a series of precipitation stages which grew the seed from 60 µm to 100-105 µm. Two sets of precipitation conditions were used, namely initial ratios of 0.500 and 0.650 respectively. After each stage the attrition strength and size distribution of the product were determined.

Results summarized in Tables 5 and 6, and illustrated in Figure 6, show that the attrition indices on the hydrate product decreases continuously as the product is coarsened. However, this decrease is nonlinear and levels off when the size of product reaches 80-85 µm. It appears also that the attrition index on the hydrate is mainly a function of the size of the product and, at constant product size, is not affected by the initial precipitation ratio. The attrition indices on the corresponding calcined products exhibit a quite different evolution. In particular the attrition indices of products obtained at low supersaturation, i.e. 0.500 initial ratio, increase dramatically when the size is increased beyond 80 µm. The increase is less pronounced and occurs only at 100 µm for products precipitated at 0.650 ratio. Note that the fines balances show that more fines are generated in the tests carried

Table 5. Attrition Strength with Consecutive Coarsening Cycles at 0.500 Initial Ratio

| Cycle | 0 (seed) | 1 | 2 | 3 | 4 | 5 | 6 |
|---|---|---|---|---|---|---|---|
| Yield ($g/L\ Al_2O_3$) | - | 24.8 | 26.2 | 25.2 | 23.9 | 22.7 | 22.8 |
| Median (μm) | 61 | 66 | 72 | 79 | 89 | 94 | 101 |
| Area ($m^2/g$) | 0.043 | 0.039 | 0.035 | 0.032 | 0.028 | 0.026 | 0.021 |
| Population Balances | | | | | | | |
| $N/g \times 10^{-6}$ | 5.1 | 3.8 | 3.2 | 1.9 | 1.2 | 1.7 | 1.2 |
| $N/L \times 10^{-6}$ | - | -50 | -110 | -250 | -140 | 90 | -90 |
| Attrition (%) | | | | | | | |
| Hydrate | 17.7 | 13.0 | 7.6 | 4.9 | 4.6 | 4.5 | 3.2 |
| Alumina | 44.5 | 37.7 | 37.7 | 28.6 | 29.9 | 32.8 | 35.9 |

Table 6. Attrition Strength With Consecutive Coarsening Cycles at 0.650 Initial Ratio

| Cycle | 0 (seed) | 1 | 2 | 3 | 4 |
|---|---|---|---|---|---|
| Yield ($g/L\ Al_2O_3$) | - | 52.9 | 58.1 | 55.9 | 56.2 |
| Median (μm) | 61 | 73 | 87 | 101 | 106 |
| Area ($m^2/g$) | 0.043 | 0.035 | 0.032 | 0.023 | 0.025 |
| Population Balances | | | | | |
| $N/g \times 10^{-6}$ | 5.1 | 3.5 | 4.9 | 1.9 | 6.3 |
| $N/L \times 10^{-6}$ | - | 40 | 200 | -600 | 1000 |
| Attrition (%) | | | | | |
| Hydrate | 17.7 | 6.8 | 3.2 | 3.0 | 3.5 |
| Alumina | 44.5 | 30.5 | 19.5 | 18.9 | 20.5 |

out at high initial ratio. This is consistent with previous results on the effect of the initial ratio. As shown in Tables 5 and 6, fines generation seems to occur by bursts when the seed is too coarse, or when the seed surface area is too small; e.g. small amounts of fines are generated with a seed of 94 μm for precipitation at 0.500 ratio while significantly more fines are generated with a seed of 87 μm and 106 μm for precipitation at 0.650 ratio.

The observed differences in the variation in attrition strength of the products, obtained at low and high ratios, as a function of particle size suggest that the fragility of the coarse material is not so much related to mass of the particles (i.e. higher momentum during attrition) but rather to the morphology of the particles produced. The SEM photomicrographs of the products obtained at 0.500 and 0.650 ratio and with product sizes of ≃ 100 μm (i.e. after the 5th and 3rd cycle respectively) presented in Figure 7, confirm this point. Products obtained at low supersaturation consist of large monocrystals with little fill-up between the individual grains, while the products obtained at high supersaturation have a more rounded appearance with more fill-up between the individual grains. As evidenced by the small nuclei present

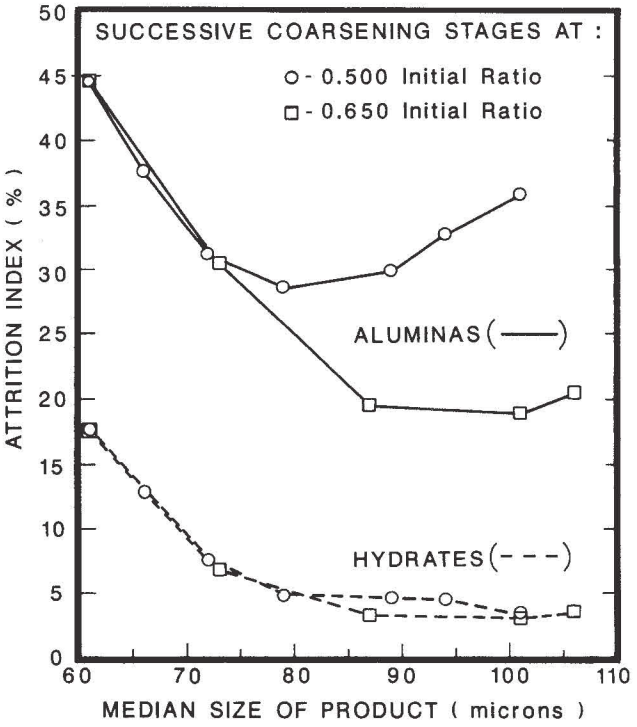


Figure 6. Evolution of the Attrition Strength of Product With Increasing Size Through Successive Coarsening Stages

on the surface, this difference in morphology can be again explained by a surface nucleation phenomenon occurring at high supersaturation.

SEM examinations of the calcined products after attrition indicate that the product obtained at low supersaturation exhibits many more gross fractures and produces larger amounts of small fragments than the product obtained at high supersaturation. Particle size analysis of the product before and after attrition reported in Table 7, show that these attrited products obtained at low supersaturation contain considerably more fines than the product obtained at high supersaturation, e.g. 7.7% - 20 μm vs 2.6% - 20 μm.

Table 7. Particle Size Distribution of Calcined Product Before and Afer Attrition

| Precipitation Ratio | Percent Less Than (μm) | | | | | | | | | | |
|---|---|---|---|---|---|---|---|---|---|---|---|
| | 20 | 30 | 40 | 45 | 60 | 70 | 80 | 90 | 100 | 120 | Quartile Spread (μm) |
| 0.500* | 0.1 | 0.2 | 1.0 | 1.0 | 10.3 | 44.6 | 74.2 | 97.5 | 99.5 | 100 | 14 |
| | 7.7 | 17.1 | 23.5 | 31.9 | 40.6 | 62.5 | 84.0 | 97.6 | 99.1 | 100 | 32.1 |
| 0.650* | 0.1 | 0.4 | 0.5 | 0.6 | 1.6 | 15.3 | 42.4 | 80.8 | 97.2 | 100 | 14 |
| | 2.6 | 7.5 | 11.6 | 15.8 | 22.4 | 45.2 | 71.8 | 95.1 | 99.3 | 100 | 19.5 |

* First Line before attrition, second line after attrition. Product from the 5th cycle at 0.500 ratio and from the 3rd cycle at 0.650 ratio

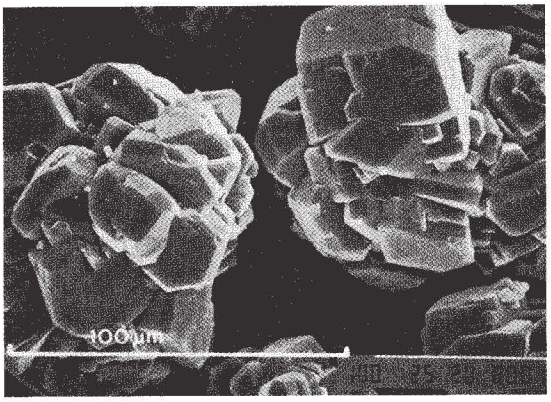


(A)

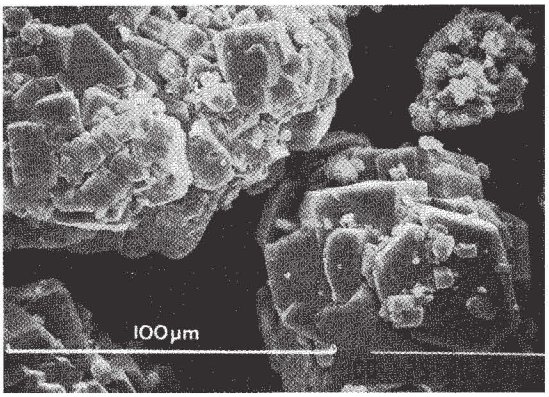


(B)

Figure 7. Products Obtained at Low and High Ratios in Successive coarsening Cycles (a) 0.500 ratio, 5th Cycle (b) 0.650, 3rd Cycle.

It was found that the attrition indices of plant product generally follow the same trend as outlined in the case of laboratory prepared products. As shown for example in Table 8 for one product from the Alcan group's plants the attrition index on the hydrate decreases continuously as the size increases while the attrition index on the corresponding laboratory calcined product passes through a minimum and then increases significantly with the coarsest fraction.

Table 8. Attrition as a function of Particle Size for a Plant Product

| Size Fraction (µm) | 45-74 | 74-105 | 105-150 |
|---|---|---|---|
| (%) | 12.2 | 42.4 | 41.5 |
| Attrition Indices | | | |
| Hydrate | 6.2 | 3.0 | 2.5 |
| Alumina | 20.9 | 15.1 | 23.6 |

## CONCLUSIONS

This work has established that the strength of the product is related to the mode of crystal growth: strong products are obtained at high liquor supersaturations conducive to growth by a surface nucleation mechanism which tends to fill-up the space between crystallites with a "cementing" layer of hydrate. Therefore, strong products are obtained under conditions which increase the supersaturation level, i.e. low precipitation temperatures, high initial ratios and decreased caustic concentrations. The evolution of the attrition strength during a precipitation cycle confirms the importance of the degree of liquor supersaturation: strengthening occurs only in the early stage of a precipitation cycle where the supersaturation level is higher than 30 g/L. It appears that such a threshold level is related to the energy barrier required for the generation of surface nuclei[6].

The results obtained on the decreased attrition strength of the calcined product obtained by overcoarsening an agglomerated seed have an important bearing on plant operation. For maximum strength the agglomerated seed should be coarsened in a maximum of three consecutive coarsening cycles; overcoarsening results in large blocky monocrystals which result in weak calcined products.

## ACKNOWLEDGEMENT

The author wishes to thank Mr. G. Bekmesian for his contribution to this work.

## REFERENCES

1. W. Stählin, J. Bachmann and S. Molnar, "Alumina Morphology and Particle Strength", Light Metals 1985, 423-433.

2. H.P. Hsieh, "Morphological analysis of Alumina and its trihydrate", Light Metals 1985, 397-423.

3. D.J. Braun, "Attrition of Aluminas", Light Metals 1984, 257-269.

4. J.V. Sang, "Continuous Precipitation Simulation", Light Metals, 1986, 191-198.

5. W.L. Forsythe and W.R. Hertwig, "Attrition Characteristics of Fluid Cracking Catalysts, Ind. and Eng. Chem., 41 (1949), 1200-1206.

6. B. Simon and R. Boistelle, "Crystal Growth from Low Temperature Solutions", Journal of Crystal Growth, 52 (1981), 779-788.